LASER ACCELERATION AND LASER COOLING FOR ION BEAMS

M. Roth, A. Blazevic, E. Brambrink, M. Geissel, University of Technology Darmstadt, Germany
T.E. Cowan, J. Fuchs, A. Kemp, H. Ruhl, University of Nevada, Reno, NV, USA
P. Audebert, Laboratoire pour l'Utilisation des Lasers Intense, Palaiseau, France
J. Cobble, J. Fernandez, M. Hegelich, S. Letzring, Los Alamos National Laboratory, NM, USA
K. Ledingham, P. McKenna, University of Strathclyde, Glasgow, United Kingdom
R. Clarke, D. Neely, S. Karsch, Rutherford Appleton Laboratory, Didcot, United Kingdom
D. Habs, U. Schramm, M. Bussmann, J. Schreiber, Ludwigs Maximilian Universität, München, Germany

Abstract

Cooling and acceleration of ions by lasers has gained increasing attention over the last years. The common interest is to further increase the luminosity of ion beams, either by shrinking the phase space occupied by the beam, or simply via increasing the number of particles. Recently, laser cooling has demonstrated ion beam crystallization as the ultimate reduction of the beam temperature. On the other hand, acceleration of ions by ultra-intense lasers resulted in the generation of ion beams of unprecedented quality, both in terms of beam power and beam emittance.

LASER COOLING

The cooling of stored heavy ion beams to high phase space densities is of general importance when low momentum spread is required for precision spectroscopy or high luminosity for collision experiments. Ultimately, cooling the thermal energy far below the mutual Coulomb energy leads to a phase transition, a crystallization of the ion beam, into a regime where almost no further heating occurs and maximum brilliance is reached. This state is up to now only reached for low energy beams of singly charged Mg ions by laser cooling in a small scale storage ring [1-3] and for extremely dilute beams of highly charged ions subject to electron cooling (see refs in [3]). For higher energies shear forces and the insufficient symmetry of existing storage rings inhibited the transition, a situation that can possibly be overcome with the GSI FAIR project where laser cooling of ion beams of highly charged heavy ions is planned [3].

Electron cooling as the established tool for ion beam cooling cannot be used for highly relativistic beams. In this regime laser cooling, though untested under these conditions, is expected to provide the possibility for an improvement of the beam quality. For counter propagating laser and ion beams the photon energy is Doppler shifted in the rest frame of the ion thereby allowing for tuning those photons into resonance with ground state transitions of Li-like systems. An advantage arises from the general increase of the laser cooling force with γ^3 in the lab frame. The momentum of the reemitted photon is increased by $4\gamma^2$ and the lifetime of the excited level is shortened roughly proportional to γ. For cooling, the momentum dependent laser force has to be counteracted by the restoring force of a bunching cavity. As ions perform synchrotron oscillations inside the corresponding bucket, the momentum acceptance of the laser force has to be matched to the momentum distribution inside the bucket. Otherwise ions are only cooled on a fraction of their oscillation resulting in considerably increasing cooling times.

The electronic transition used for laser cooling only provides a small momentum acceptance, a fact that principally allows for the cooling to extremely low momentum spread. Thus, pulsed lasers with increased bandwidth and spectral power will be used to address this task of fast cooling of an initially broad distribution.

At the GSI heavy ion storage ring ESR a test experiment for combined electron and laser cooling of relativistic C^{3+} beams at an energy of 1.4 GeV has recently been performed as an intermediate step towards the cooling of highly relativistic beams at the FAIR facility. Though in this first test only a narrow band laser was used beams of about 10μA bunched at the 20^{th} harmonic could be laser cooled into the space charge dominated regime and to an unprecedented momentum spread of the order of $\Delta p/p \approx 1\ 10^{-7}$ corresponding to a plasma parameter of order unity. A more detailed analysis of the experiment including the cooling dynamics is presently in progress. As the next step the use of a laser beam that is better matched to the momentum spread of the ion beam is planned as well as studies of sympathetic cooling of other ion species like O^{4+}. Regarding the preliminary results of the C^{3+} experiment, for the highly charged relativistic U^{89+} beam a dramatic improvement of the equilibrium momentum spread as compared to the else uncooled beam can be expected

LASER ACCELERATION

Charged particles accelerated up to energies of several MeV have been observed from laser plasma interaction for more than 20 years. Early experiments with long pulse (several nanoseconds) lasers incident on thin foils and wires observed protons and multiply charged ions

accelerated up to velocities of 10^9 cm/s. It was shown that these protons and carbons were present regardless of target material due to hydrocarbon contaminants inside the vacuum system [4].The acceleration mechanism was shown to be the result of an electrostatic field due to charge separation in the underdense region of the expanding plasma. The maximum ion acceleration correlated strongly with hot electron temperature.

In contrast to the experiments using long pulse lasers, ions accelerated by ultra-intense, fs-laser systems are emitted predominantly from the rear, non-irradiated surface in a low divergent beam of excellent quality [5]. The dominant mechanism is understood as rear surface emission by the TNSA (Target Normal Sheath Acceleration) mechanism and published in detail in [6]. Briefly, relativistic electrons generated from the laser plasma interaction, having an average temperature of several MeV, envelope the target foil and form an electron plasma sheath on the rear, non-irradiated surface. The electric field in the sheath ($E_{stat} \sim kT_{hot}/e\lambda_D$, $\lambda_D = (\varepsilon_0 kT_{hot}/e^2 n_{e,hot})^{1/2}$) can reach $> 10^{12}$ V/m. A few monolayers of atoms at the rear surface are field-ionized and accelerated normal to the surface by E_{stat} with the most energetic electrons always extending further out into the vacuum, maintaining the accelerating field as long as the electron temperature is high. Because of the accompanying electrons, the ion beam is space charge and current neutralized. So far mainly protons have been observed from the rear surface, originating from contaminating hydrocarbon and water vapour layers which coat the target. The ions form a collimated beam with an approximately exponential energy distribution with 5-6 MeV. The conversion efficiency from laser energy to ion beam energy can be quite high and efficiencies of order of 10 % have already been measured [5]. Because of the dependence of the ion beam on the formation of the electron sheath, this process should also reveal information about the electron transport through the target. As will be shown below, the extreme strong, transient acceleration that takes place from a cold, initially unperturbed surface, results in the low beam emittance that may be limited only by the collisions with the comoving electrons during the acceleration. Such an acceleration process represents a new and potentially near-ideal kind of ion diode as compared either to the ion beams generated from plasma plumes, i.e., from the laser-heated turbulent plasma on the front side of the foils, or to the conventional plasma discharge ion sources used in accelerators.

EXPERIMENTS

We have studied the influence of the target properties on laser-accelerated ion beams generated by multi-terawatt lasers. The experiments were performed using the 100 TW laser facility at Laboratoire pour l'Utilization des Laser Intense (LULI), at the 30 TW Trident laser at the Los Alamos National Laboratory, and at the 1000 TW Vulcan laser at Rutherford Appleton Laboratory. The targets were irradiated by pulses up to 5×10^{19} W/cm^2 (~ 300 fs, λ=1.05μm) at normal incidence. To characterize the plasma conditions and ion beam parameters, we used short pulse laser interferometry, absolutely calibrated ion spectrometers, Radio-chromic film (RCF), CR-39 nuclear track detectors, nuclear activation, neutron time-of-flight diagnostics, and Thomson Parabolas to detect heavy ions with respect to their charge-to-mass ratio. Stacking the RCF and CR-39 provided spatial beam profile information at different ion energies. Details of the experimental setup and the various diagnostics were published in [7].

RESULTS

We performed a series of experiments to examine the properties of the laser accelerated ion beam. The majority of the accelerated ions on regular targets were found to be protons, as mentioned in the introduction. Those protons, originating from surface contaminants outrun all other ion species due to their higher charge-to-mass ratio and screen the accelerating field thereby gaining most of the energy stored in the field. The energy distribution resembles an exponential spectrum up to a sharp cut-off energy, in our experiments at about 25 MeV. The angular dependence of the energy distribution was measured with two ion spectrometers, positioned at an angle of 0° and 13° respectively. The maximum energy of about 25 MeV dropped to about 13 MeV at 13° normal to the target rear surface, consistent with the data from the RCF-stack. Details about the spectral distribution have been published in [8]. The ion beam pulse duration has been estimated to 10 ps as an upper limit due to the finite lifetime of the accelerating electrons [9], but recent measurements using accelerated heavy ions provided more accurate data, indicating individual, much shorter pulse durations for different ion species[10], well within the limits published in [9].

One of the interesting features of the laser accelerated ion beams is their directionality always normal to the rear surface. Structures at the target rear surface strongly influence the spatial distribution of the ion beam, as published in [7]. We have shown that beam tailoring by appropriate target design is possible, including defocusing and focusing of proton beams. In addition to the structure of the target, the imprint of the laser beam at the front surface can cause a deformation of the electron distribution at the rear surface, affecting the ion beam formation. In recent experiments we demonstrated that a strongly astigmatic focus can form an ion beam, where the orientation of the beam ellipse is perpendicular to the laser spot, consistent with numerical simulations based on the TNSA mechanism. An example is shown in figure 1, where we used an astigmatic focus to generate an elliptical proton beam from a flat target.

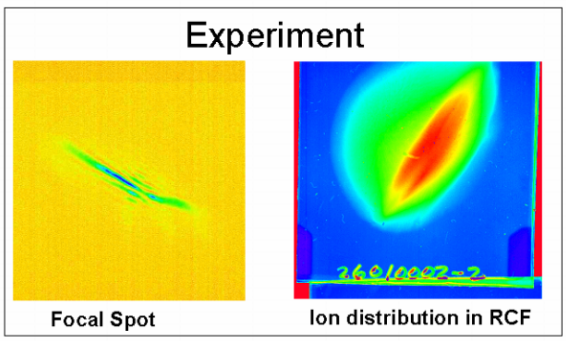

FIGURE 1. Effect of laser imprint on the ion beam shape for a strongly astigmatic laser focal spot.

For future applications of laser generated ion beams the beam quality is the most important characteristic. Especially for the use as an ion source or the application as an inertial fusion (ICF) ignitor beam[11], the ion beam emittance is crucial. As is apparent from the radiochromic film data the angular divergence of the beam is rather well defined and decreases with increasing proton energy. This suggests that the protons or other light ions accelerated by this mechanism may have a usefully small emittance in the sense of an actual ion beam.

Using a new technique that allows one to directly image the initial accelerating sheath and to fully reconstruct the transverse phase space, we have shown experimentally that, for protons of up to 10MeV, the transverse emittance is as low as 0.004 mm mrad, i.e., 100-fold better than typical RF accelerators and at a substantially higher ion current (kA range)[12]. In addition, the removal of the comoving electrons after 1 cm of beam expansion does not increase significantly the measured proton transverse emittance. This was the first demonstration of high-current laser-produced charged-particle beams with characteristics substantially superior to conventional accelerators. Also, we determined directly for the first time the size of the ion source, a crucial parameter for developments of high-resolution charged-particle radiography or ion patterned lithography.

The technique we developed for imaging the accelerating sheath uses a target design that allows manipulating the ion beam generation during the initial, virtual cathode phase of the acceleration by generating a stream of beamlets, within the expanding proton envelope, that can be used as fiducials of the acceleration.

The laminarity of charged-particle beams is characterized by their emittance [13], which is proportional to the volume of the bounding ellipsoid of the distribution of particles in phase space. By Liouville's theorem, the phase-space volume of a particle ensemble is conserved during nondissipative acceleration and focusing. For the transverse phase-space dimensions (here x-p_x for beam propagation along z), the area of the bounding phase space ellipse equals $\pi\varepsilon_N$, where the root-mean-square (rms) value of the ''normalized emittance'' ε_N, at a specific beam energy (or momentum p), is expressed as $\varepsilon_N=(|p|/mc)[<x^2><x'^2>-<xx'>^2]^{1/2}$, where m is the ion mass, c is the velocity of light, x is the particle position within the beam envelope, and $x'=p_x/p_z$ *is* the particles' divergence in the x direction.

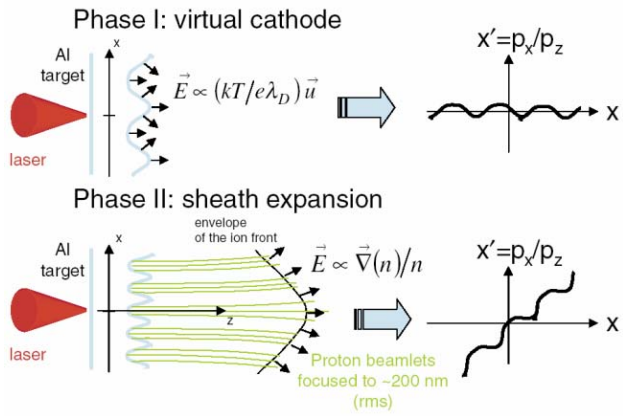

FIGURE 2: Schematic of experiment. The laser pulse is focused on a foil having a modulated rear surface. Protons are first accelerated normal to the surface by the virtual cathode (VC) producing a modulation of the takeoff angle. The produced beamlets then expand with the quasineutral sheath. This adds an overall near-linear divergence to the beam initial angular modulation. Projected on a film stack far away, this results in a modulation of the dose, allowing one to image the VC stage magnified.

At the beam waist, we have $\varepsilon_N=\beta\gamma\sigma_x\sigma_{x'}$, where σ_x and $\sigma_{x'}$ are the rms values of the beam-width and divergence angle. For typical proton accelerators [e.g., the CERN Super Proton Synchrotron (SPS)], the emittance from the proton injector linac is ~1 mm mrad (normalized rms) and up to 3.5 mm mrad within the synchrotron, with 10^{11} protons per bunch. The longitudinal phase space (z-p_z) is characterized by the equivalent, energy-time product of the beam envelope and a typical value, for the CERN SPS, is ~0.5 eVs. The highest quality ion beams have the lowest values of transverse and longitudinal emittance, indicating a low effective transverse ion temperature and a high degree of angle-space and time-energy correlation.

The concept of the experiment is shown schematically in Fig. 2. Laser pulses of ~20–200 J of 1 μm light (350– 850 fs) were focused onto the front surface of thin foils of Au or Al (10–50 μm thick). Note that the targets can be used only once since they are destroyed during the shot.

The accelerated protons are detected in multiple layers of radiochromic film (RCF) densitometry media [14]. The spatial distribution of the protons in a given RCF layer gives the angular emission pattern at a specific interval of proton energy. By carefully preparing the rear surface of the target foil, and by shaping the laser focal intensity distribution, we controlled the virtual-cathode phase of the acceleration where the electric field is normal to the ion charge layer [15,16]. For the data of Figs. 3(a)–3(c),

we used optically flat aluminium foils on the rear surface of which we micromachined shallow grooves, 200 nm deep spaced 3.6 μm apart. From a quantitative analysis of the film optical densities, we measure that ~10^{11} protons are produced in a single laser shot for energies above 4 MeV, which corresponds to an ion current of >1 kA at 1 mm from the target foil. We observe a decrease in the angular envelope of the protons with increasing proton energy, as has been observed previously [5,7]. However, using the modulation of the beam intensity impressed during the initial phase, we are able to image the proton-emitting surface and thus to measure for the first time directly the source size. By accelerating protons off non-periodic surface structures we verified that there is no overlap of the beam fiducials from adjacent structures that could lead to misinterpretation of the data.

By assuming that the protons in each beamlet come from an ideal line focus, we experimentally deduce an upper limit on the transverse emittance of <0.004 mm mrad for 10 MeV protons, a factor of >100 smaller than typical proton beam sources. We attribute this to the fact that during much of the acceleration the proton space charge is neutralized by the comoving hot electrons. PIC simulations show that the image generation is more complicated.

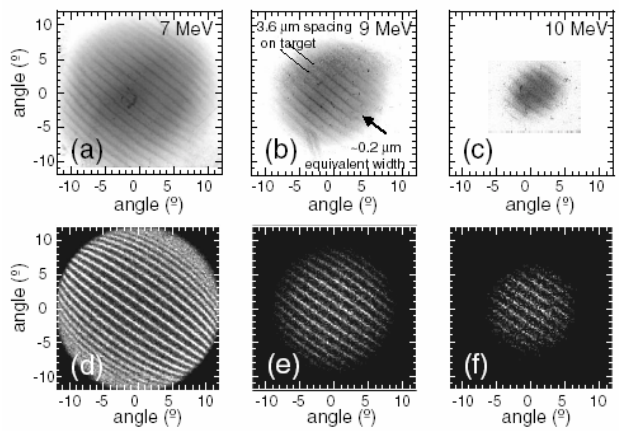

FIGURE 3:. (a) –(c) Angular distributions on RCF of protons accelerated from an 18 _m thick Al flat target irradiated at 10^{19} W=cm^2. (d) –(f) Simulated RCF images [same parameters and proton energies as in (a) –(c)] using a 3D PIC effective code.

The energy spread of the laser-accelerated proton beam is large, ranging from 0–10 MeV; however, due to the extremely short duration of the accelerating field (<10 ps), the longitudinal phase-space energy-time product must be less than 10^{-4} eVs. The 3D PIC simulations show that longitudinally the acceleration is extremely laminar, in the sense that the spread of proton energies in a given longitudinal slice is very small. We estimate from the simulation an energy-time product of <10^{-7} eVs. Such extremely good longitudinal velocity "chirp" of the beam is interesting since it could in principle allow one to monochromatize a portion of the beam by coupling it to the field gradient of a post-accelerator.

HEAVY ION ACCELERATION

So far mainly protons have been observed from the rear side, originating, as in the long-pulse experiments, from contaminating hydrocarbon layers which coat the targets. As soon as protons are present they outrun the heavier ions and screen the acceleration field. We present the experimental study, demonstrating that besides protons, also high-quality, high energy (~MeV/nucleon) heavy ion beams can be accelerated from the rear surface of (coated) thin foils. We find that heavy ions are effectively accelerated, provided that the hydrogenous surface contaminants are removed.

We obtained high resolution, absolutely calibrated energy spectra of different ion species, which provide additional information, not available in the proton signal, about the spatio-temporal evolution of the accelerating field and the origin of the observed ions. Details on the acceleration of heavy ions are published in [10]. To effectively remove the hydrogen contaminants we resistively heated tungsten targets up to temperatures of 1000 K for several minutes. The ion species of interest was coated solely on the rear surface of the target, thereby unambiguously verifying the origin of the heavy ions. The proton spectrometer as well as the CR-39 did not show any protons, while strong fluorine ion tracks are observed originating from the CaF_2 layer at the target rear side. The complete removal of contaminants increased the acceleration of heavier ions considerably. Quantitative evaluation shows that F^{7+} was accelerated up to 100MeV, i.e. more than 5MeV/nucleon at 4% energy conversion. The RCF diagnostic confirmed this by showing a narrow spot in the first layer, which, in the absence of protons, indicates fluorine ions of energies above 4MeV/nucleon. The evaluation of the fluorine shot shows that E-fields E_{stat} ~ 2TV/m on a time scale of τ ~350fs are necessary to accelerate F^{7+}-ions up to 100MeV over a scale length of l ~10 μm. The shot presented in Fig.6 was virtually without any protons, but the modeled fields can accelerate protons up to ~25MeV, as typical with unheated targets. The field distribution is in agreement with an extended TNSA model including dynamic fields and multiple ion species. We found that field ionization is the dominant mechanism while recombination and collisional ionization are by far less effective (see [10]). Since the targets were coated only at the back surface and we successfully removed contaminations we can rule out front side acceleration within the parameters of our experiment.

Furthermore, recent experiments using structured, coated and heated targets, have shown the heavy ion beam quality (emittance) to be comparable to the proton beam quality.

APPLICATIONS

The excellent beam quality of the ion beam is ideally matched to the requirements for imaging techniques. One scheme of particular interest is the use of laser accelerated protons to radiograph macroscopic samples to study their properties. Due to the different interaction mechanism protons can provide complementary information to techniques like x-ray backlighting. Because of the copious amounts of protons accelerated in a very short time, laser accelerated protons provide a new diagnostic quality in research of transient phenomena.

We performed experiments to demonstrate the feasibility of these laser accelerated proton beams for radiography applications. In our experiments, we used a compound target of different materials to be imaged by the protons. It consisted of an 1 mm thick epoxy ring structure, several copper wires of 250 µm diameter, a hollow cylinder with 300 µm walls of steel, several Ti sheets of 100 µm thickness and a glass hemisphere of 900 µm diameter and 20 µm wall thickness. The protons were recorded in multiple layers of RCF to detect the image at different proton energies.

Fig.4 shows the radiography of the target for final proton energies of 7.5 MeV. The picture basically constitutes a negative image of the areal density of the target. The names of the collaborating institutes have been engraved on the epoxy ring, which results in a reduced thickness and therefore a higher energy deposition of the protons in the respective layer.

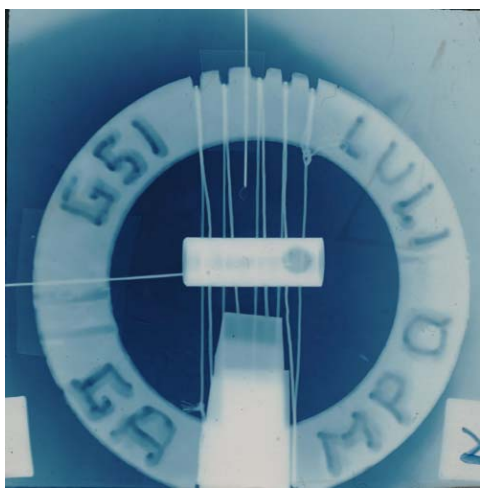

FIGURE 4. Radiography of a compound target. Details of the target are given in the text.

The areal density variation of the hollow cylinder, including a hole in the wall on the right hand side can be seen as well as a thin metal rod placed inside the cylinder. Close examination also shows the small glass hemisphere placed above the cylinder. The time of exposure in this experiment was estimated to be in the order of tens of picoseconds.

CONCLUSION:

Laser accelerated proton and ion beams offer new prospects for a whole variety of applications. The beam quality was found to be far superior to beams accelerated by conventional accelerators with respect to the transversal beam emittance, while the longitudinal phase space was found to be comparable. The beam intensity exceeds present accelerators by orders of magnitude. The excellent beam quality implies a highly laminar acceleration and an initially extremely cold beam and the experiments proved the beam to have optical qualities. The properties are highly interesting for applications, especially as we have shown the possibility of tailoring the beam with respect to shape, ion species, efficiency, and homogeneity. A wealth of applications are currently being investigated, starting from improved diagnostic capabilities [17], to industrial and medical applications, to next generation ion sources and prospects for fast ignition in inertial confinement fusion [11,18]. Still the underlying physics is subject to further investigation and, with respect to the extensive interest, future improvements are likely to be developed in the next years.

We acknowledge the expert support of the LULI, Trident and VULCAN laser teams.

This work was supported by the EU Contract No. HPRI CT 1999-0052, and in part by grant E1127 from Region Ile-de-France, LANL Laboratory Directed Research & Development, corporate support of General Atomics and UNR Grant No. DE-FC08-01NV14050.

REFERENCES

[1] T. Schätz, et al., Nature 412 (2001) 717
[2] U. Schramm et al., Proc.PAC 2003, TOAA004 (2003)
[3] U. Schramm, D. Habs, Prog. Part. Nucl. Phys.(2004)
[4] S.J. Gitomer et al., Phys. Fluids 29, 2679 (1986)
[5] R. Snavely, et al., Phys. Rev. Lett. **84**, 640 (2000)
[6] S. C. Wilks, et al., Phys. Plasmas **8**, 542 (2001)
[7] M. Roth, et al., Phys. Rev. ST-AB 5,061301
[8] M. Allen, et al., Phys. Plasmas,**10**, 3283 (2003)
[9] S. Hatchett, et al., Phys. Plasmas **7**, 2076 (2000)
[10] M. Hegelich, et al., Phys. Rev. Lett.**89**, 85002 (2002)
[11] M. Roth, et al., Phys. Rev. Lett. **86**, 436 (2001)
[12] T.E. Cowan, et al., Phys.Rev.Lett. **92**, 204801 (2004)
[13] S. Humphries, Charged Particle Beams (Wiley, New Jersey, 1990)
[14] N.V. Klaasen, et al., Med. Phys. **24**, 1924 (1997)
[15] H. Ruhl, et al., Phys. Plasmas **11**, L17 (2004)
[16] J. Fuchs, et al., Phys. Rev. Lett., **91**, 255002 (2003)
[17] M. Borghesi, et al., Plasma Phys and Contr. Fusion **43** A267
[18] M. Temporal, et al., Phys. Plasmas **9**, 3098 (2002)